Chemical Engineering Journal 149 (2009) 249–262

Contents lists available at ScienceDirect

Chemical Engineering Journal

journal homepage: www.elsevier.com/locate/cej

Removal of lead(II) from wastewater by activated carbon developed from *Tamarind wood* by zinc chloride activation

Jyotikusum Acharya[a], J.N. Sahu[b], C.R. Mohanty[c], B.C. Meikap[b,*]

[a] *School of Energy and Environment Management, Rajib Gandhi Technical University (RGTU), Gandhinagar, Bhopal, Madhya Pradesh, India*
[b] *Department of Chemical Engineering, Indian Institute of Technology (IIT), Kharagpur, P.O. Kharagpur Technology, Kharagpur, West Bengal 721302, India*
[c] *State Pollution Control Board, Orissa, Bhubaneswar, India*

ARTICLE INFO

Article history:
Received 19 August 2008
Received in revised form 13 October 2008
Accepted 30 October 2008

Keywords:
Lead removal
Activated carbon
Chemical activation
Zinc chloride
Adsorption
Wastewater treatment

ABSTRACT

In this work, the adsorption of lead(II) was studied on activated carbon prepared from *Tamarind wood* with zinc chloride activation. Adsorption studies were conducted in the range of 10–50 mg/l initial lead(II) concentration and at temperature in the range of 10–50 °C. The experimental data were analyzed by the Freundlich isotherm and the Langmuir isotherm. Equilibrium data fitted well with the Langmuir model and Freundlich model with maximum adsorption capacity of 43.85 mg/g. The rates of adsorption were found to confirm to pseudo-second-order kinetics with good correlation and the overall rate of lead(II) uptake was found to be controlled by pore diffusion, film diffusion and particle diffusion, throughout the entire adsorption period. Boyd plot confirmed that external mass transfer was the rate-limiting step in the sorption process. Different thermodynamic parameters, viz., ΔH°, ΔS° and ΔG° have also been evaluated and it has been found that the sorption was feasible, spontaneous and endothermic in nature. The results indicate that the *Tamarind wood* activated could be used to effectively adsorb lead(II) from aqueous solutions.

1. Introduction

Lead is a heavy, soft, malleable, bluish gray metal. Its common ore is galena where it occurs in the form of sulphide. Most of the lead in the air comes as aerosols, fumes and sprays. It is very widely used in din storage batteries and the gasoline auto exhaust from gasoline. Powder motor vehicle is the major source of atmospheric layer in the urban area. Other anthropogenic sources of lead include the combustion of coal, processing and manufacturing of lead products and manufacturing of lead additives such as tetra ethyl lead (TEL) for gasoline. Some lead is also introduced in the atmospheric during incineration of refuse of lead containing pesticides. Lead is systemic poison causing anemia, kidney malfunction, tissue damage of brain and even death in extreme poison. Lead occurs as its sulphide, cerussite ($PbCl_2$) and galena. Lead is also present at 50 parts per million (ppm) in the earths crust. In sea water 5 parts per billion (ppb) lead is present. It is found in all living organism. Those it is distributed in food and in environment. A human body contains about 121 ppb, 96% in the bone. The concentration of lead increases with age and it may reach to a limit at 400 mg. It is not essential for mammals. Under specific condition lead is stimulatory causing enhancing of protein synthesis, DNA synthesis and cell replication. Any metabolic disturbance resulting is an osteolysis will liberate lead from its skeletal storage. Lead is deposited mostly in bones and in some soft tissues. Lead is also retaining by mammals in lever, kidney, muscles, etc. About 800 mg of lead create toxicity in human beings. The removal Pb(II) from industrial effluents is a major problem due to the difficulty in threating such waste waters by conventional treatment method. The presence of lead in waste water is dangerous to aquatic flora and fauna even in relatively low concentration and stringent environmental regulation attracts the attention of chemists and environmental engineers for its control. The major sources containing lead are the waste water from process industries engaged in lead acid battery, paints, oils, mental phosphate, fertilizer, electronic wood production and also combustion of fossil fuel, forest fires, mining activity, automobile emission, sewage waste water, sea spray, etc. are just few examples [1–3]. The industrial wastewaters are considered to be the main source of lead impurities.

The presence of high levels of lead in the environment may cause long-term health risks to humans and ecosystems. It is there fore mandatory that their levels in drinking water, waste water and water used for agricultural and recreational purposes must be reduced to within the maximum allowable concentrations recom-

* Corresponding author. Tel.: +91 3222 283958 (O)/2283959 (R); fax: +91 3222 282250.
E-mail addresses: bcmeikap@che.iitkgp.ernet.in, bcmeikap@iitkgp.ac.in (B.C. Meikap).

1385-8947/$ – see front matter © 2008 Elsevier B.V. All rights reserved.
doi:10.1016/j.cej.2008.10.029

Nomenclature

$1/n$	sorption intensity (dimensionless)
b	Langmuir constant (l/g)
C_e	equilibrium lead(II) concentration (mg/l)
C_0	initial lead(II) concentration (mg/l)
D_i	effective diffusion coefficient (m^2/s)
d_p	diameter of the adsorbent particles (mm)
F	represents the fraction of solute adsorbed at any time t (mg/g)
ΔG°	free energy of sorption (kJ mol^{-1})
ΔH°	heat of sorption (kJ mol^{-1})
k	measure of adsorbent capacity (l/g)
K	the constant obtained by multiplying K_L and b (Langmuir's constants) (mg l/g^2)
K_2	equilibrium rate constant of pseudo-second-order adsorption (min^{-1})
K_{ad}	equilibrium rate constant of pseudo-first-order adsorption (min^{-1})
K_c	equilibrium constant (dimensionless)
k_{id}	rate constants of intraparticle diffusion (mg/g $min^{-1/2}$)
K_L	Langmuir constant (mg/g)
M	mass of the adsorbent per unit volume (g/l)
q_e	amount of lead(II) adsorbed at equilibrium (mg/g)
R	radius of the adsorbent particles (μm)
S_s	outer specific surface of the adsorbent particles per unit volume of particle free slurry (g/m^3)
ΔS°	standard entropy (kcal mol^{-1} K^{-1})
T	temperature (°C)
t	time (min)
V	volume of the solution (l)
W	weight of adsorbent (g)

Greek letters

β_1	mass transfer coefficient (cm s^{-1})
δ_ρ	density of the adsorbent particles (g/l)
ε_p	porosity of the adsorbent particles (m Dc)

mended by national and international health authorities such as World Health Organisation (WHO). Its removal from wastewater prior to discharge into environment is, there fore, necessary. Current EPA drinking water standard for lead are 0.05 mg/l, but a level of 0.02 mg/l has been proposed and is under review [4]. According to Indian Standard Institution (ISI), the tolerance limit for discharge of lead into drinking water is 0.05 mg/l [5] and in land surface waters is 0.1 mg/l [6]. Increasingly stringent legislation on the purity of drinking water has created a growing interest in the development of conventional treatment processes. Various chemical and physicochemical methods for the treatment of wastewaters containing lead wastes are known, such as chemical precipitation, electrochemical reduction, ion exchange, biosorption and adsorption [7–11]. The choice of treatment depends on effluent characteristics such as concentration of lead, pH, temperature, flow volume, biological oxygen demand, the economics involved and the social factor like standard set by government agencies. However, adsorption on to the surface of activated carbons is the most widely used method [12–18]. Despite its prolific use in industries, activated carbon remains an expensive material. In recent years, research interest in the production of low-cost alternatives to activated carbon has grown.

Activated carbon is a black solid substance resembling granular or powder charcoal and are carbonaceous material that have highly developed porosity, internal surface area of more than 400 m^2 g^{-1} and relatively high mechanical strength [19]. They are widely used as adsorbents in wastewater and gas treatments as well as in catalysis. The increasing usage and competitiveness of activated carbon prices has prompted a considerable research work in the search of inexpensive adsorbents especially developed from various agricultural waste materials i.e. the usage of agricultural by-products such as fruit stones [20,21], coconut shell [22,23], bagasse [24,25], nutshells [26,27] and coirpith [28,29] rice husk [30] as raw materials to prepare AC. These solid wastes are not only cheap and easily available but also are considered as wastes that contribute to disposal problems. In this study *Tamarind wood* was chosen as an adsorptive media, as it is suitable for preparing microporous activated carbon due to its excellent natural structure and low ash content.

Most of the activated carbons are produced by a two-stage process carbonization followed by activation. The first step is to enrich the carbon content and to create an initial porosity and the activation process helps in enhancing the pore structure. Basically, the activations are two different processes for the preparation of activated carbon: physical activation and chemical activation. There are two important advantages of chemical activation in comparison to physical activation. One is the lower temperature in which the process is accomplished. The other is that the global yield of the chemical activation tends to be greater since burn off char is not required. Among the numerous dehydrating agents, zinc chloride in particular is the widely used chemical agent in the preparation of activated carbon [31]. Knowledge of different variables during the activation process is very important in developing the porosity of carbon sought for a given application. Chemical activation by zinc chloride improves the pore development in the carbon structure, and because of the effect of chemicals, the yields of carbon are usually high [32].

In this work it has been reported the results obtained on the preparation of activated carbon from *Tamarind wood* with zinc chloride activation and their ability to remove lead(II) from waste water. The influence of several operating parameters for adsorption of Pb(II), such as contact time, initial concentration, temperature, pH, particle size, adsorbent dose, etc. were investigated in batch mode. The kinetic data were fitted to different models and the isotherm equilibrium data were fitted to Langmuir and Freundlich.

2. Experimental technique

2.1. Adsorbate

A stock solution of Pb(II) was prepared (1000 mg/l) by dissolving required amount of, $Pb(NO_3)_2$ in distilled water. The stock solution was diluted with distilled water to obtain desired concentration ranging from 20 to 60 mg/l. All the chemicals used in the study were from Merck (India) Ltd. and Qualigens Glaxo (India) Ltd. analytical grade.

2.2. Adsorbent: Tamarind wood activated

The *Tamarind wood* was collected from Indian Institute of Technology campus of Kharagpur, West Bengal, India and washed with deionized water four to five times for removing dirt and dust particles. The washed wood was cut into 50.8–76.2 mm pieces. The woods were sun dried for 20 days. Chemical activation of the precursor was done with $ZnCl_2$. 10 g of dried precursor was well mixed with distilled water so that 100 ml concentrated solution contained 10 g of $ZnCl_2$. The chemical ratio is defined as the ratio of chemical activating agent ($ZnCl_2$) to the precursor. The chemical ratio (activating agent/precursor) was 100% in this case. The

mixing was performed at 50 °C for 1 h. After mixing, the slurry was subjected to vacuum drying at 100 °C for 24 h. The resulting chemical-loaded samples were placed in a stainless-steel tubular reactor and heated (5 °C/min) to the final carbonization temperature under a nitrogen flow rate of 150 ml/min STP. Samples were held at the final temperature (carbonization temperature) for carbonization times of 40 min before cooling down under nitrogen. Nitrogen entering in the reactor was first preheated to 250–300 °C in a pre-heater. The products were washed sequentially with 0.5N HCl, hot water and finally cold distilled water to remove residual organic and mineral matters, then dried at 110 °C. In all experiments, heating rate and nitrogen flow was kept constant. The experiments were carried out for chemical ratio of (296%), activation time (40 min) and carbonization temperature (439 °C) this was the optimization condition find out using response surface methodology. Then carbon was dried to 60 °C. After this, carbon was crushed in a small ball mill with 50 numbers of small balls for 1 h. The powder from ball mill is collected and dried to remove the moisture. Then this powder carbon was kept in airtight packet for the experimental use.

2.3. Method of experiment

Batch adsorption experiments were performed by contacting 0.2 g of the selected activated samples with 100 ml of the aqueous solution of different initial concentration (10, 20, 30, 50 mg/l) at natural solution pH (5.68). The experiments were performed in a thermal shaker at controlled temperature (30 ± 2 °C) for a period of 1 h at 120 rpm using 250 ml Erlenmeyer flasks containing 100 ml of different lead(II) concentrations at room temperature. Continuous mixing was provided during the experimental period with a constant agitation speed of 120 rpm for better mass transfer with high interfacial area of contact. The remaining concentration of Pb(II) in each sample after adsorption at different time intervals was determined by atomic-absorption spectroscopy after filtering the adsorbent with Whatmen filter paper to make it carbon free. The batch process was used so that there is no need for volume correction. The lead(II) concentration retained in the adsorbent phase was calculated according to

$$q_e = \frac{(C_i - C_e)V}{W} \quad (1)$$

where C_i and C_e are the initial and equilibrium concentrations (mg/l) of lead(II) solution respectively; V is the volume (l); and W is the weight (g) of the adsorbent. Two replicates per sample were done and the average results are presented.

The effect of adsorbent dosages (1–5 g/l) on the equilibrium adsorption of Pb(II) on the selected carbon was investigated by employing different initial concentrations (10, 20, 30 and 50 mg/l) at different temperature (10–50 °C). For these experiments, the flasks were shaken, keeping the pH at natural (6.2) constant and agitation speed (120 rpm) for the minimum contact time required to attain equilibrium, as determined from the kinetic measurements detailed above.

2.4. Analytical method

Atomic-absorption spectrophotometry utilizes the phenomenon that atoms absorb radiation of particular wavelength. By atomic-absorption spectrophotometer, the metals in water sample can be analyzed. It detect concentration of Pb(II) in ppm level in the solution and volume of sample required is only 1 ml for one analysis.

2.5. Characterization of the prepared activated carbon

2.5.1. Pore structure characterization

The pore structure of the precursor and modified carbons were analyzed using N_2 adsorption, X-ray diffraction (XRD), and scanning electron microscope (SEM). The BET surface area, total pore volume and density functional theory (DFT) pore size distribution were determined from nitrogen adsorption/desorption isotherms measured at −194 °C (boiling point of nitrogen gas at atmospheric pressure) by a Quantachrome Autosorb-I. Prior to gas adsorption measurements, the activated carbon was degassed at 200 °C in a vacuum condition for a period at least 4 h. The BET surface area was determined by means of the standard BET equation applied in the relative pressure range from 0.05 to 0.3. The total pore volume was calculated at a relative pressure of approximately 0.98 and at this relative pressure all pores were completely filled with nitrogen gas. The DFT pore size distribution of activated carbon sample was obtained based on nitrogen adsorption isotherms, using Autosorb software package with medium regularization.

Powder X-ray diffraction (XRD) patterns were recorded on a Rigaku Miniflex Goniometer at 30 kV and 15 mA (Cu Kα radiation). Scanning electron microscopy (SEM) analysis was carried out on the activated carbon prepared under optimum conditions, to study its surface texture and the development of porosity. In this study, SEM Images were recorded using JEOL JSM-6300F field emission SEM. A thin layer of platinum was sputter-coated on the samples for charge dissipation during SEM imaging. The sputter coated was operated in an argon atmosphere using a current of 6 mA. The coated samples were then transferred to the SEM specimen chamber and observed at an accelerating voltage of 10 kV, 8 spot size, 4 aperture and 5 mm working distance.

2.5.2. Surface chemistry determination

The surface chemistry of the precursor and modified carbons were determined using Fourier transform infrared radiation (FTIR). FTIR analysis was applied on the same activated carbon to determine the surface functional groups, by using FTIR spectroscope (FTIR-2000, PerkinElmer), where the spectra were recorded from 400 to 4000 cm^{-1}.

2.5.3. Particle size analysis

Particle size analysis of powder activated carbon samples was done on using a Malvern instruments, mastersizer 2000 (UK). Samples were dispersed in water with the help of an ultrasonic magnetic stirrer before feeding into the instrument. Through use of laser diffraction technology, the technique of laser diffraction is based around principle that particles passing through a laser beam will scatter light at an angle that is directly related to their size. As the particle size decreases, the observed scattering angle increases logarithmically.

3. Results and discussions

3.1. Physical and chemical characterization of the adsorbent

3.1.1. Chemical properties

Adsorbent pH may influence the removal efficiency. Distinctly acidic adsorbent may react with the material to be removed and may hamper the surface properties of the adsorbent. The pH of activated Tamarind wood was measured by using the method recommended by Al-Ghouti et al. [33] as follows: 3 g of activated carbon was mixed with 30 ml of distilled water and agitated for 24 h. Then the pH value of the mixture was recorded with a pH meter. For our experiment the pH of activated Tamarind wood was 6.77.

Table 1
Physico-chemical characteristics of the activated *Tamarind wood*.

Parameters	Values
Moisture (%)	10
Ash (%)	4.55
Volatile matter (%)	36.48
Fixed carbon (%)	48.97
Bulk density (g/ml)	0.791
BET surface area (m^2/g)	1322
Total pore volume (cm^2/g)	1.042
Mean pore radius (Å)	5.3

Ash content of the activated carbon is the residue that remains when the carbonaceous portion is burned off. The ash consists mainly of minerals such as silica, aluminum, iron, magnesium and calcium. Ash in activated carbon is not required and considered to be an impurity. Table 1 shows the proximity analysis of activated Tamarind wood. As the ash content is 4.55% it resembles good adsorbent.

The spectra of the prepared activated carbon were measured by an FTIR spectrometer within the range of 400–4000 cm^{-1} wave number. The FTIR spectrum obtained for the prepared activated carbon and adsorbed Pb(II) plotted was shown in Fig. 1.

3.1.2. Physical properties

The smaller the particle sizes of a porous carbon, the greater the rate of diffusion and adsorption. Intraparticle diffusion is reduced as the particle size reduces, because of the shorter mass transfer zone, causing a faster rate of adsorption. Since we have prepared our carbon in a powdered form so it has a great efficiency of removal. The particle size analysis of the prepared activated carbon was done using Malvern analyzer. From Fig. 2 it shows that there are no particles above the size of 150 μm.

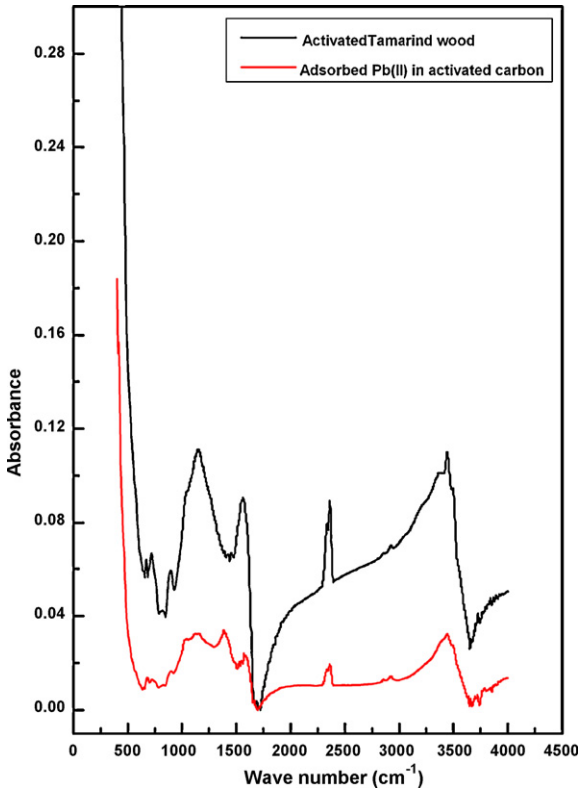

Fig. 1. FTIR result of prepared activated carbon and adsorbed with Pb(II).

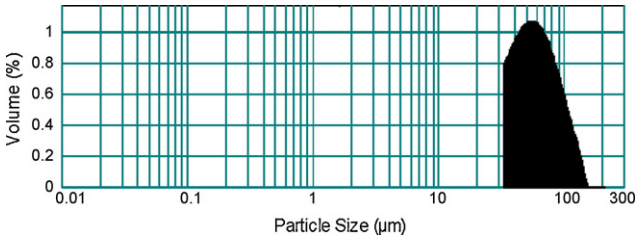

Fig. 2. Particle size distribution of activated *Tamarind wood* measured using Malvern Master Size.

Density is particularly important in removal. If two carbons differing in bulk density are used at the same weight per liter, the carbon having higher bulk density will be able to remove more efficiently. Average bulk density can be calculated by water displacement method. In this method, volume of water displaced is observed by a particular amount of carbon. The average bulk density was found 0.791 g/ml.

From the N_2 adsorption–desorption isotherms as shown in Fig. 3(a) and (b), it was possible to obtain the specific BET surface areas and the pore size distributions shown in Fig. 4(a) and (b), the precursor (raw *Tamarind wood*) and the activated carbon. The activated carbon exhibit, type I and type IV isotherms. Type I isotherm corresponds to essentially microporous activated carbon, and type IV isotherm indicates the presence of mesoporosity leading to a gradual increase in adsorption after the initial filling of the micropores type I isotherm. The isotherms have two characteristics regions; at low-pressure region ($P/P_0 < 0.2$) significant uptake of nitrogen occurred. This means that nitrogen molecules are adsorbed in the microporous structure. The adsorption in micropores was interpreted according to the pore filling mechanism, thus result in highly adsorbed volume. While at higher relative pressure ($P/P_0 > 0.2$), smaller gas volume adsorbed with increased relative pressure. This indicates the existence of type IV isotherm. Surface area and total pore volume of activated carbon is also obtained from N_2 adsorption isotherm. The surface area and total pores volume for the activated carbon is found to be 1322 m^2/g and 1.042 cm^3/g, respectively. The DFT result is given in Fig. 4(b) and it shows that the activated carbon consists mainly pore width from 5 to 60 Å.

Fig. 5 shows the scanning electron microscope (SEM) images of the activated carbon obtained under the optimum preparation conditions. There was very little pores available on the surface of the precursor. However, after $ZnCl_2$ treatment under the optimum preparation conditions, many large pores in a honeycomb shape were developed on the surface of the activated carbon and a smooth melt surface appeared, interspersed with generally large pores due to some of the volatiles being evolved as shown in Fig. 5.

The XRD result in Fig. 6 shows the crystalline structure of the carbon layers of prepared activated carbon, under the optimum preparation conditions at 500 °C activation temperature, 1 h activation time and 200% impregnation ratio. There are two broad peaks that are common to activated carbon, namely (0 0 2) and (1 0) peaks. The two broad peaks observed near $2\theta = 24^\circ$ and 42° are assigned to the (0 0 2) and (1 0) reflections.

3.2. Lead adsorption

3.2.1. Contact time study

The relationship between contact time and lead sorption onto activated Tamarind wood at different initial lead concentrations is shown in Fig. 7. The adsorption was very fast from the beginning to 30 min and the adsorption capacities increased from 78 to 91% with the lead concentration range of 10–50 mg/l at a

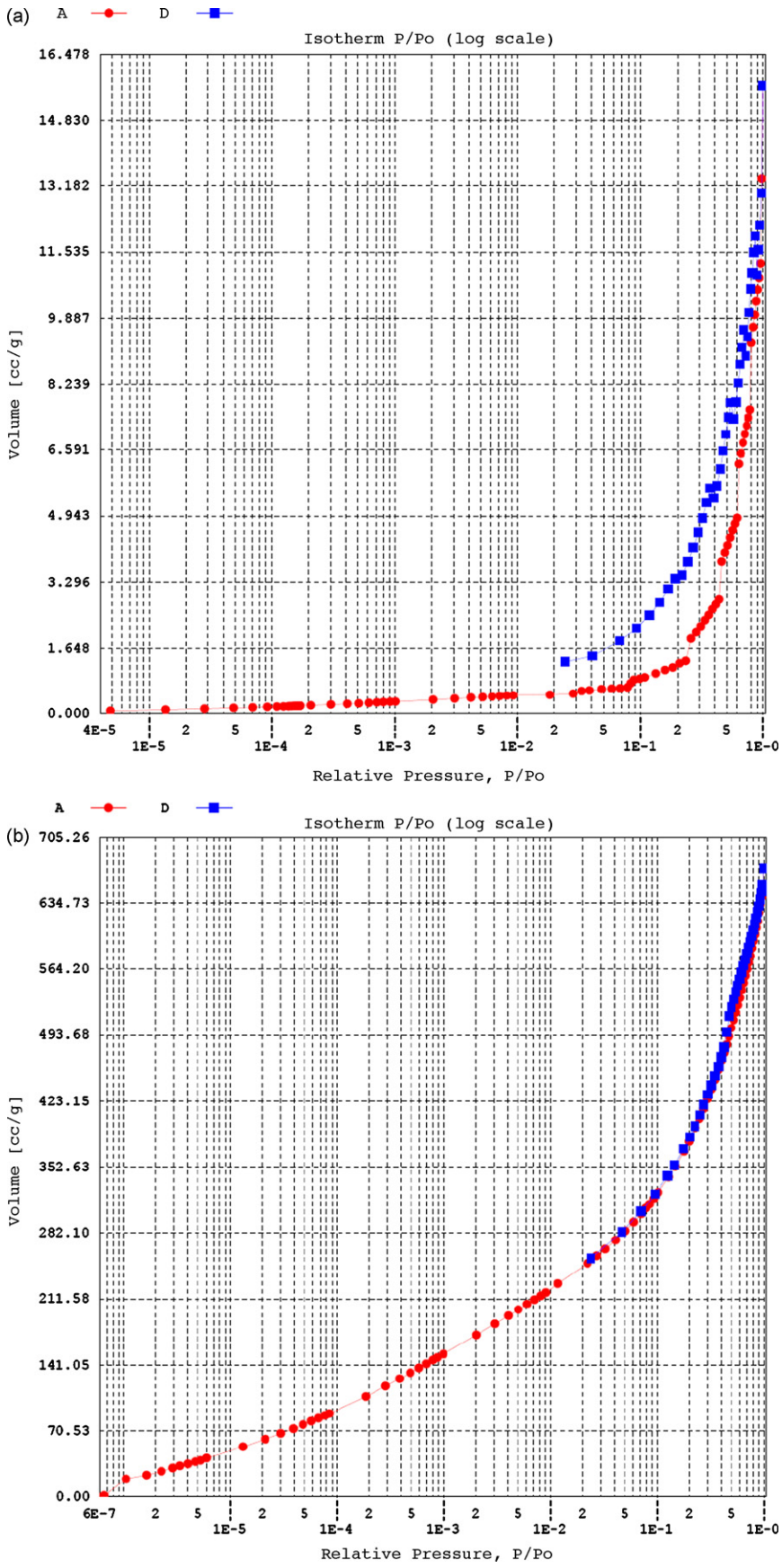

Fig. 3. (a) N_2 adsorption/desorption isotherm of precursor (raw *Tamarind wood*). (b) N_2 adsorption/desorption isotherm of prepared activated carbon.

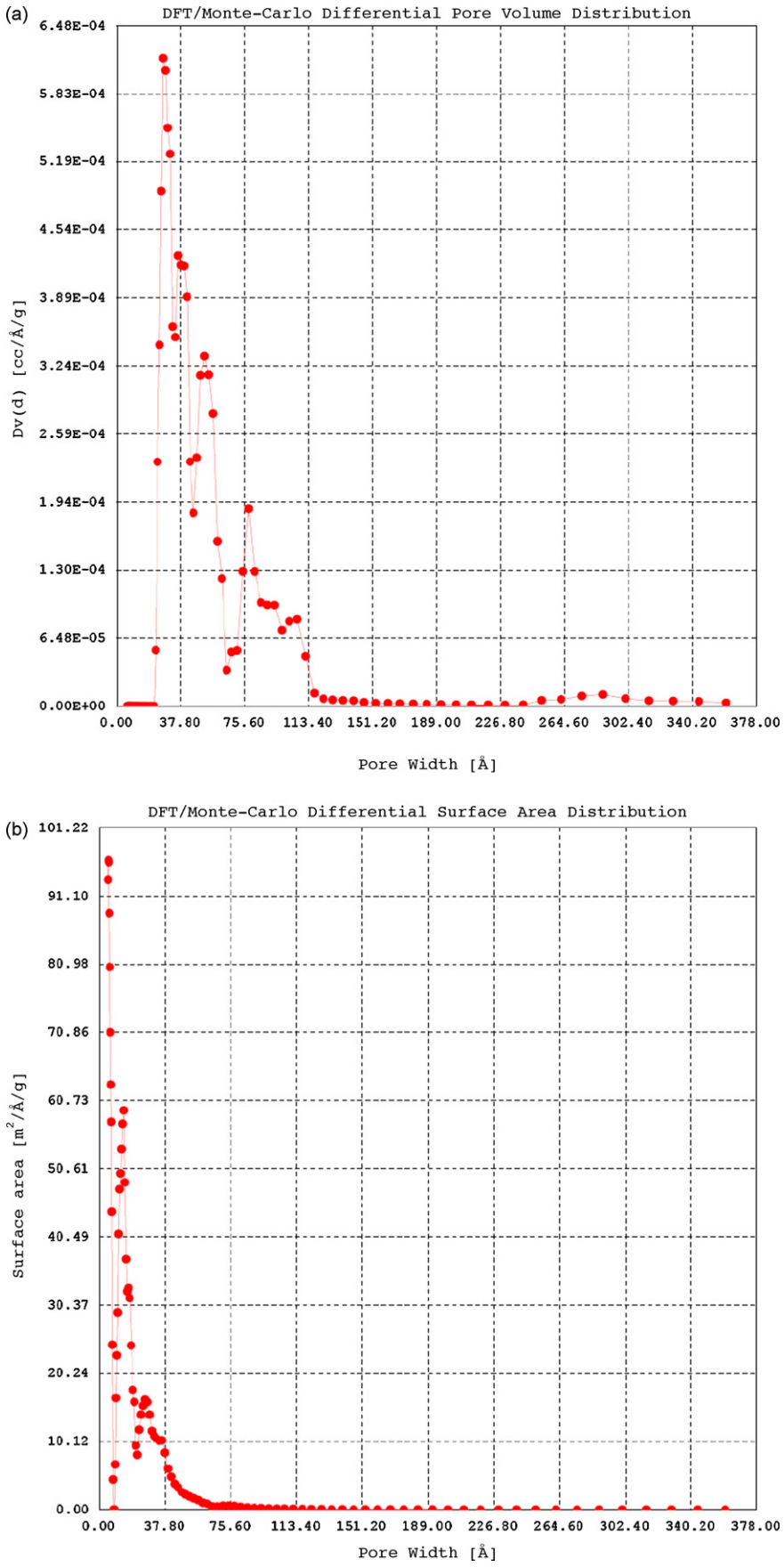

Fig. 4. (a) Determination of pore size distribution of precursor (raw *Tamarind wood*) using DFT. (b) Determination of pore size distribution of prepared activated carbon using DFT.

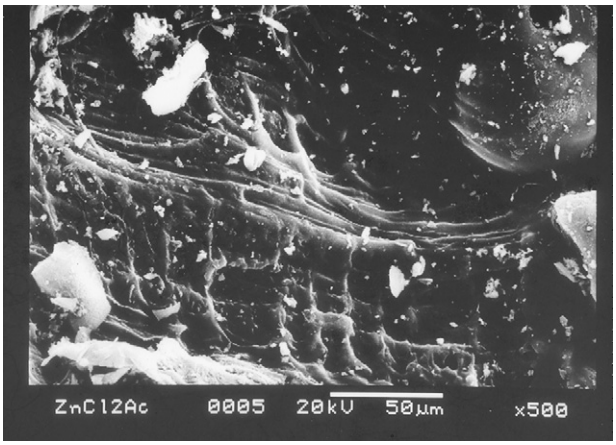

Fig. 5. Scanning electron micrograph (1000×) of prepared activated carbon.

contact time of 30 min. With further increase of time, the sorption kinetics decreased progressively, and finally the adsorption approached to equilibrium within 50 min in all the cases. The sorption capacities corresponding to equilibrium adsorption increased from 86 to 94% with the increase in lead concentration from 10 to 50 mg/l. The fast adsorption at the initial stage is probably due to the increased concentration gradient between the adsorbate in solution and adsorbate in adsorbent as there must be increased number of vacant sites available in the beginning. The progressive increase in adsorption and consequently the attainment of equilibrium adsorption may be due to limited mass transfer of the adsorbate molecules from the bulk liquid to the external surface of activated Tamarind wood, initially and subsequently by slower internal mass transfer within the activated Tamarind wood particles.

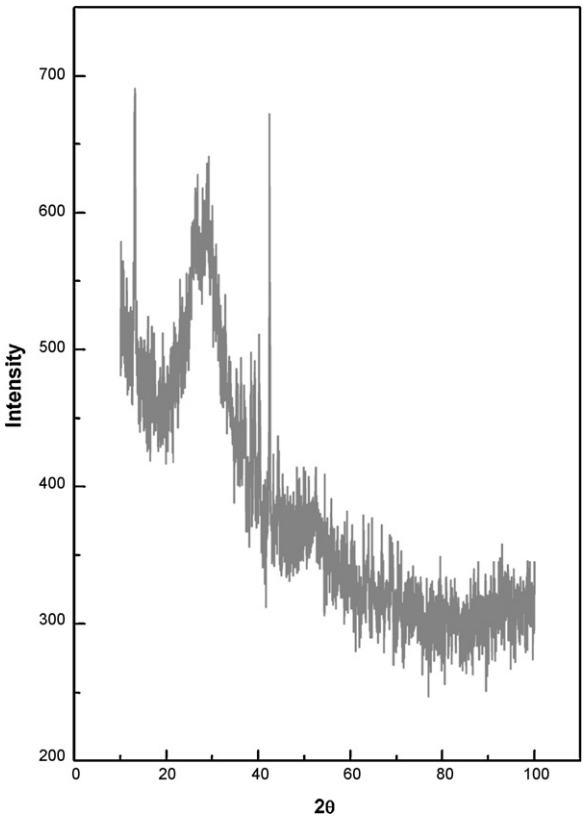

Fig. 6. X-ray diffraction result of precursor (raw *Tamarind wood*) and prepared activated carbon.

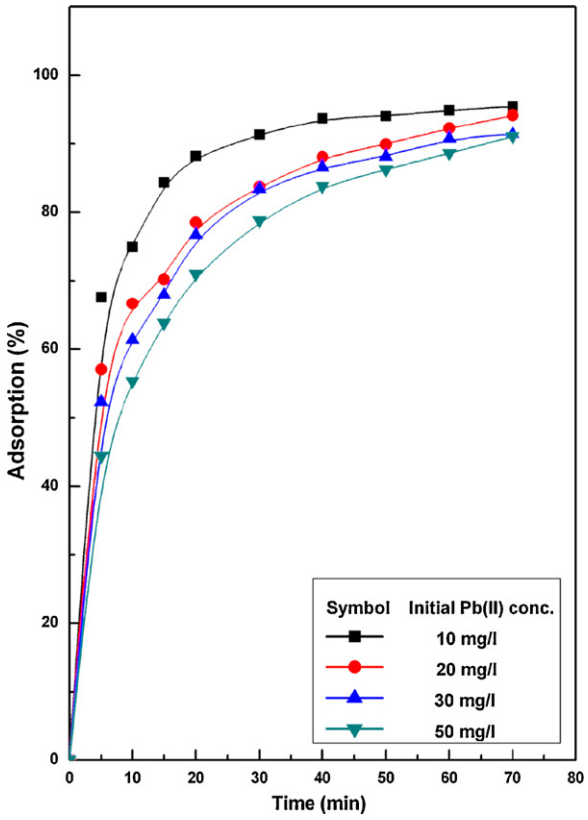

Fig. 7. Effect of contact time on adsorption of Pb(II) at different initial feed concentration and at constant temperature 30 °C, adsorbent dose 2 g/l and pH 6.5.

3.2.2. Adsorbent dose study

The effect of adsorbent dosage on the percentage removal Pb(II) has been shown in Fig. 8. It can be seen from the figure that initially the percentage removal increases very sharply with the increase in adsorbent dosage but beyond a certain value 2.5–3 g/l, the percentage removal reaches almost a constant value. This trend is expected because as the adsorbent dose increases the number adsorbent particles increases and thus more Pb(II) is attached to their surfaces. The adsorption capacities for Pb(II) increased from 88.4 to 97.7, 86.6 to 97.36 and 83.9 to 96% at 20, 30 and 50 mg/l initial feed concentration respectively with the increase in the adsorbent doses from 1 to 5 g/l at constant temperature 30 °C and pH 6.5. A maximum removal of 97.74% was observed at adsorbent dosage of 5 g/l at pH 6.5 for an initial Pb(II) concentration of 20 mg/l. Therefore, the use of 2 g/l adsorbent dose is justified for economical purposes.

3.2.3. Effect of adsorbent particle size

The influence of particle size was studied for different initial feed concentration of Pb(II) at constant temperature 30 °C and pH 6.5. Fig. 9 shows the experimental results obtained from a series of experiments performed using different particle sizes of activated Tamarind wood. The adsorption capacities for Pb(II) increased from 67 to 94, 59 to 90 and 56 to 88% at 10, 30 and 50 mg/l initial feed concentration respectively with the decrease in the particle size from 52 to 200 μm because the higher adsorption with smaller adsorbent particle may be attributed to the fact that smaller particles give large surface areas. The result showed that there was a gradual increase of adsorption with the decrease in particle size.

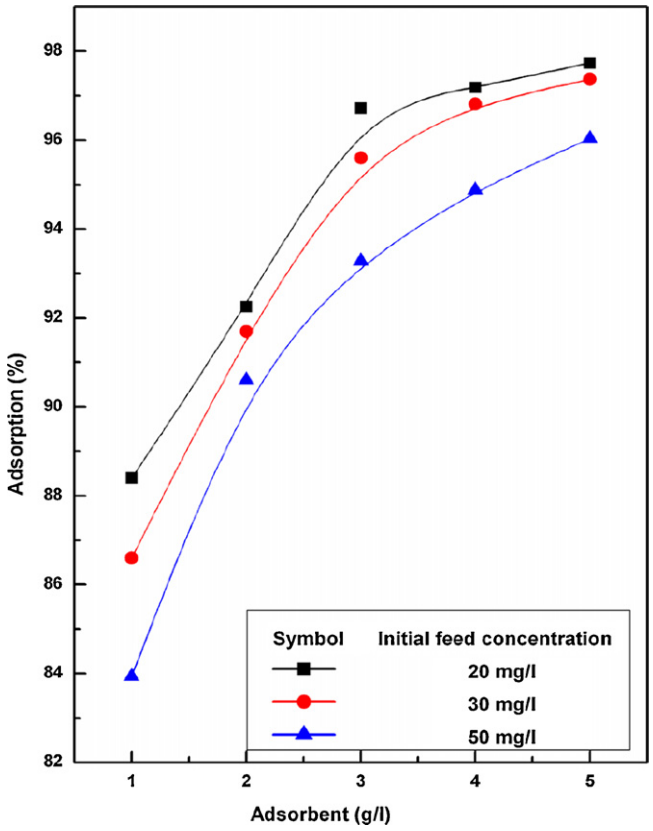

Fig. 8. Effect of adsorbent doses on adsorption of Pb(II) at different initial feed concentration and at constant temperature 30 °C and pH 6.5.

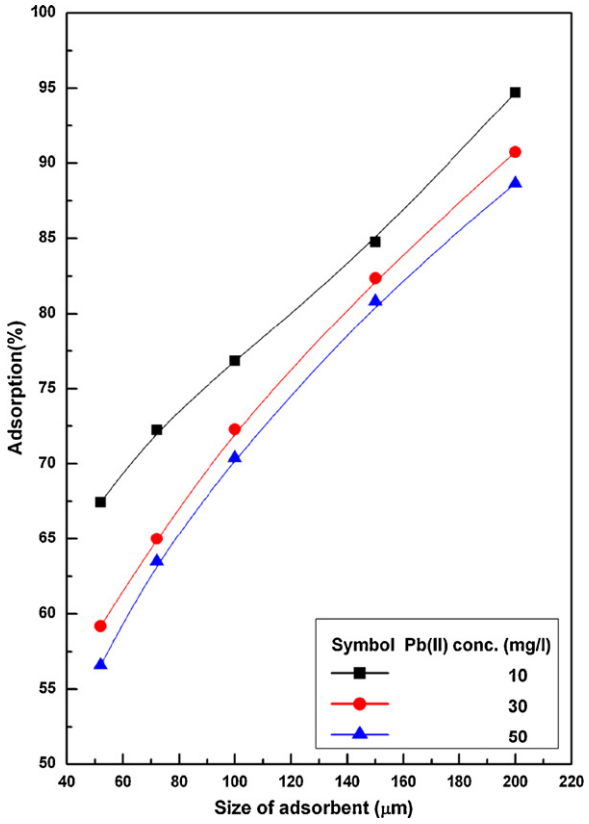

Fig. 9. Effect of size of adsorbent on adsorption of Pb(II) at different initial feed concentration at constant temperature 30 °C, adsorbent dose 2 g/l and pH 6.5.

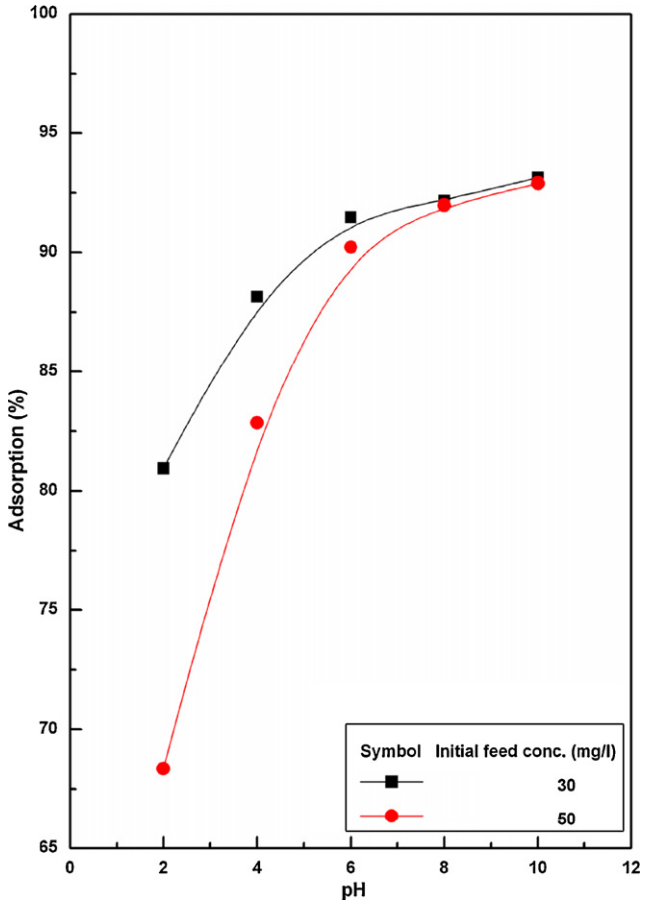

Fig. 10. Effect of pH on adsorption of Pb(II) at different initial feed concentration at constant temperature 30 °C and adsorbent dose 2 g/l.

3.2.4. *Effect of solution pH on lead adsorption*

Earlier studies have indicated that solution pH is an important parameter affecting adsorption of heavy metals. Pb(II) removal was studied as a function of pH for two different initial concentrations for a fixed adsorbent dose (2 g/l) and the results are shown in Fig. 10. It is clear from this figure that the percent adsorption of Pb(II) increases with increase in pH from pH 2.0 to 6.0 and after pH 6.5 (natural pH) no adsorption takes place at all.

3.3. *Adsorption kinetics models*

In order to investigate the controlling mechanism of adsorption processes such as mass transfer and chemical reaction, the pseudo-first-order and pseudo-second-order equations are applied to model the kinetics of lead adsorption onto activated Tamarind wood.

3.3.1. *Pseudo-first-order model*

Lagergren proposed a pseudo-first-order kinetic model. The integral form of the model is

$$\log(q_e - q) = \log\ q_e - \frac{K_{ad}}{2.303}t \quad (2)$$

where q is the amount of lead(II) sorbed (mg/g) at time t (min), q_e is the amount of lead(II) sorbed at equilibrium (mg/g), and K_{ad} is the equilibrium rate constant of pseudo-first-order adsorption (min^{-1}). This model was successfully applied to describe the kinetics of many adsorption systems.

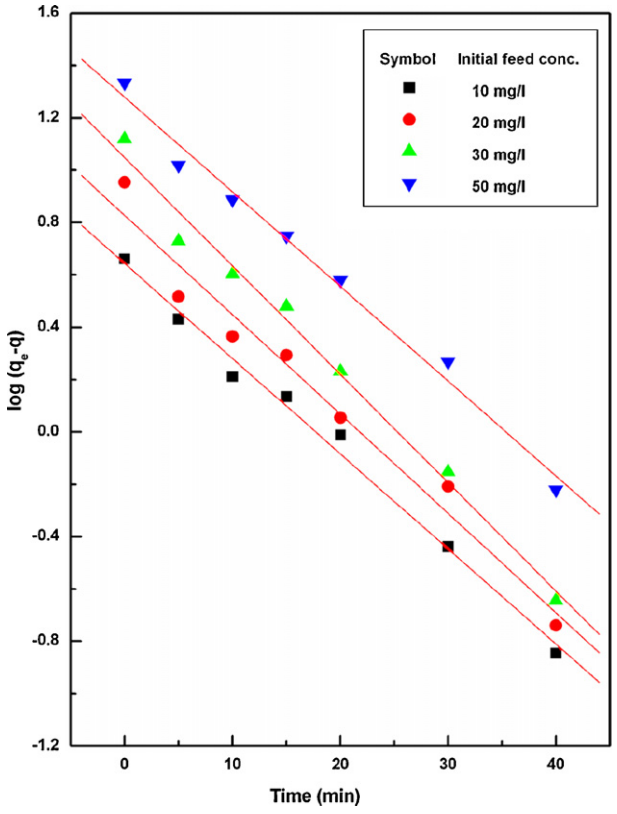

Fig. 11. Kinetics of Pb(II) removal according to the Lagergren model at initial feed concentration of 10, 20, 30 and 50 mg/l.

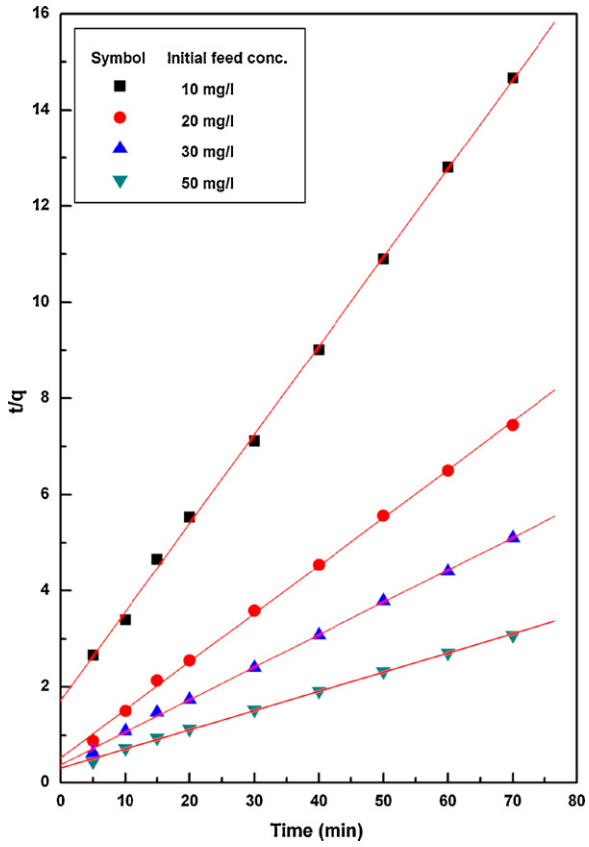

Fig. 12. Kinetics of Pb(II) removal according to the pseudo-second-order model at initial feed concentration of 10, 20, 30 and 50 mg/l.

3.3.2. *Pseudo-second-order model*

The adsorption kinetics may also be described by a pseudo-second-order reaction. The linearized-integral form of the model is

$$\frac{t}{q} = \frac{1}{K_2 q_e^2} + \frac{1}{q_e} t \tag{3}$$

where K_2 is the pseudo-second-order rate constant of adsorption.

The applicability of the above two models can be examined by each linear plot of $\log(q_e - q)$ versus t, and (t/q) versus t, respectively, and are presented in Figs. 11 and 12. To quantify the applicability of each model, the correlation coefficient, R^2, was calculated from these plots. The linearity of these plots indicates the applicability of the two models. However, the correlation coefficients, R^2, showed that the pseudo-second-order model, an indication of a chemisorptions mechanism, fits better the experimental data ($R^2 > 0.999$) than the pseudo-first-order model (R^2 is in the range of 0.985–0.995).

3.4. *Adsorption mechanisms*

It is always important to predict the rate-limiting step in an adsorption process to understand the mechanism associated with the phenomena. For a solid liquid sorption process, the solute transfer is usually characterized by either external mass transfer or intraparticle diffusion or both. Generally three types of mechanisms are involved in the adsorption process, mentioned as follows [26]:

1. Film diffusion, which involves the movement of adsorbate molecules from the bulk of the solution towards the external surface of the adsorbent.
2. Particle diffusion, where the adsorbate molecules move in the interior of the adsorbent particles.
3. Sorption of the adsorbate molecules on the interior of the porous adsorbent.

3.4.1. *Weber and Morris model*

Intraparticle diffusion model is of major concern because it is rate-determining step in the liquid adsorption systems. During the batch mode of operation, there was a possibility of transport of sorbate species into the pores of sorbent, which is often the rate controlling step. The rate constants of intraparticle diffusion (k_{id}) at different temperatures were determined using the following equation:

$$q = k_{id} t^{1/2} \tag{4}$$

where q is the amount sorbed at time t and $t^{1/2}$ is the square root of the time. The values of k_{id} (0.211, 0.591, 0.953 and 1.854 mg/g min$^{-1/2}$) at different initial feed concentrations 10, 20, 30, 50 mg/l respectively, were calculated from the slopes of respective plot (q versus $t^{1/2}$ of Fig. 13) at later stages. The dual nature of the curves was obtained due to the varying extent of sorption in the initial and final stages of the experiment. This can be attributed to the fact that in the initial stages, sorption was due to boundary layer diffusion effect whereas, in the later stages (linear portion of the curve) was due to the intraparticle diffusion effects. However, these plots indicated that the intraparticle diffusion was not the only rate controlling step because it did not pass through the origin.

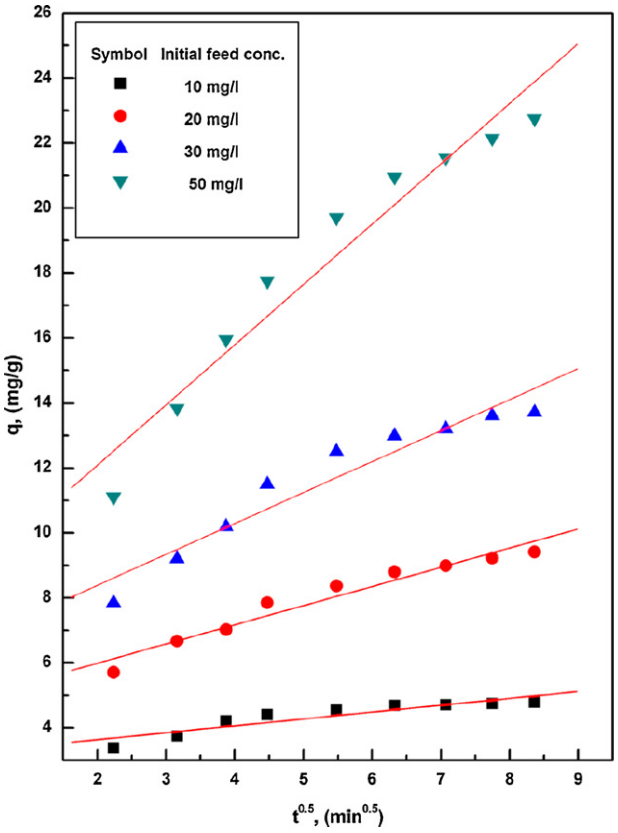

Fig. 13. Weber and Morris (intraparticle diffusion) plot for the adsorption of Pb(II) for different initial feed concentration at pH 6.5, temperature 30 °C and adsorbent dosage 2 g/l.

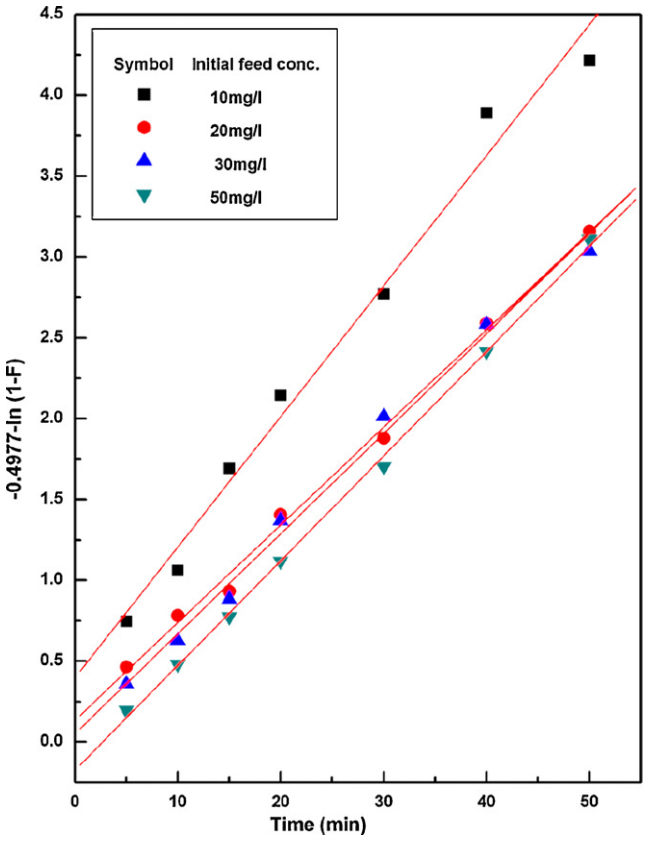

Fig. 14. Boyd plot for the adsorption of Pb(II).

3.4.2. Boyd model

Of the three steps, the third step is assumed to be very rapid and can be considered negligible. For design purposes, it is required to distinguish between film diffusion and particle diffusion. In order to identify the slowest step in the adsorption process, Boyd kinetic equation [27] was applied, which is represented as

$$F = 1 - \frac{6}{\pi^2}\exp(-Bt) \tag{5}$$

and

$$F = \frac{q}{q_e} \tag{6}$$

where q_e is the amount of Pb(II) adsorbed at equilibrium (mg/g) and q represents the amount of Pb(II) adsorbed at any time t (min), F represents the fraction of solute adsorbed at any time t, and Bt is a mathematical function of F. Eq. (5) can be rearranged by taking the natural logarithm to obtain the equation:

$$Bt = -0.4977 - \ln(1 - F) \tag{7}$$

The plot of $[-0.4977 - \ln(1 - F)]$ against time t can be employed to test the linearity of the experimental values. If the plots are linear and pass through origin, then the slowest (rate controlling) step in the adsorption process is the internal diffusion, and vice versa. From Fig. 14, it was observed that the plots are linear but do not pass though the origin suggesting that the adsorption process is controlled by film diffusion. The calculated B values were used to calculate the effective diffusion coefficient, D_i (m^2/s) using the relationship:

$$B = \frac{\pi^2 D_i}{r^2} \tag{8}$$

where D_i is the effective diffusion coefficient of solute in the adsorbent phase and r is the radius of the adsorbent particles. The D_i values were found to be 4.0×10^{-11}, 2.99×10^{-11}, 3.07×10^{-11} and 3.21×10^{-11} m^2/s, respectively for an initial Pb(II) concentration of 10, 20, 30 and 50 mg/l.

3.4.3. McKay et al. model

During the present investigation, step (2) has been assumed rapid enough with respect to the other steps and therefore it is not rate limiting in any kinetic study. Taking in to account these probable steps, McKay et al. model [28] has been used for the present investigation:

$$\ln\left(\frac{C_e}{C_0} - \frac{1}{1 + mK}\right) = \ln\left(\frac{mK}{1 + mK}\right) - \left(\frac{1 + mK}{mK}\right)\beta_1 S_s t \tag{9}$$

where m is the mass of the adsorbent per unit volume, K the constant obtained by multiplying K_L and b (Langmuir's constants), β_1 the mass transfer coefficient, and S_s is the outer specific surface of the adsorbent particles per unit volume of particle free slurry. The values of m and S_s were calculated using the following relations:

$$m = \frac{W}{V} \tag{10}$$

$$S_s = \frac{6m}{d_p \delta_\rho (1 - \varepsilon_p)} \tag{11}$$

where W is the weight of the adsorbent, V the volume of particle-free slurry solution, and d_p, δ_ρ and ε_p are the diameter, density and porosity of the adsorbent particles, respectively. The values of β_1 (2.825×10^{-4}, 3.233×10^{-4}, 6.301×10^{-4} and 8.998×10^{-4} cm s^{-1}) calculated from the slopes and intercepts of the plots (Fig. 15) of $\ln(C_e/C_0 - (1/1 + mK))$ versus t (min) at different initial feed concentration of Pb(II) (10, 20, 30 and 50 mg/l). The values of β_1 obtained

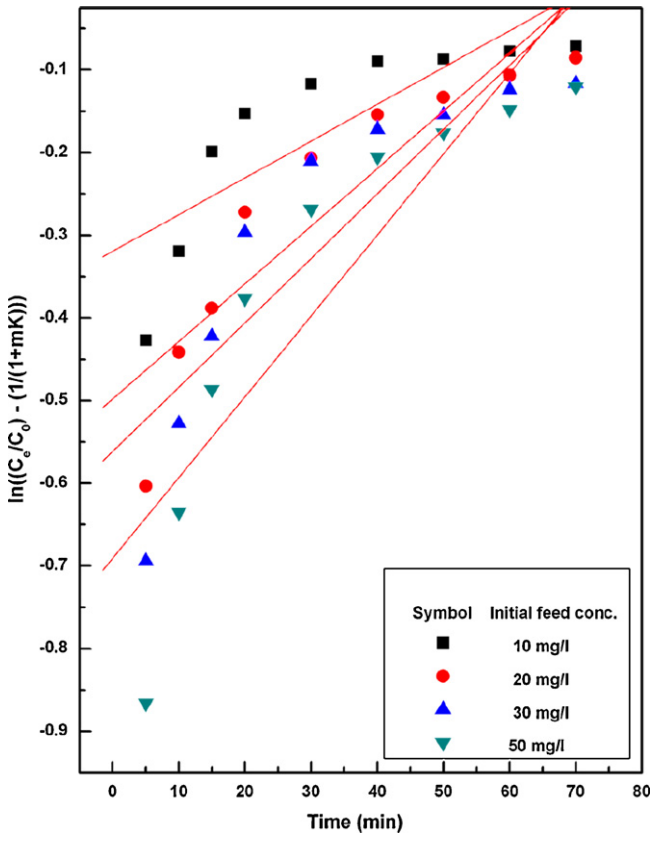

Fig. 15. Mass transfer plot for the adsorption of Pb(II) at pH 6.5, initial concentration 50 mg/l, and adsorbent dosage 2 g/l.

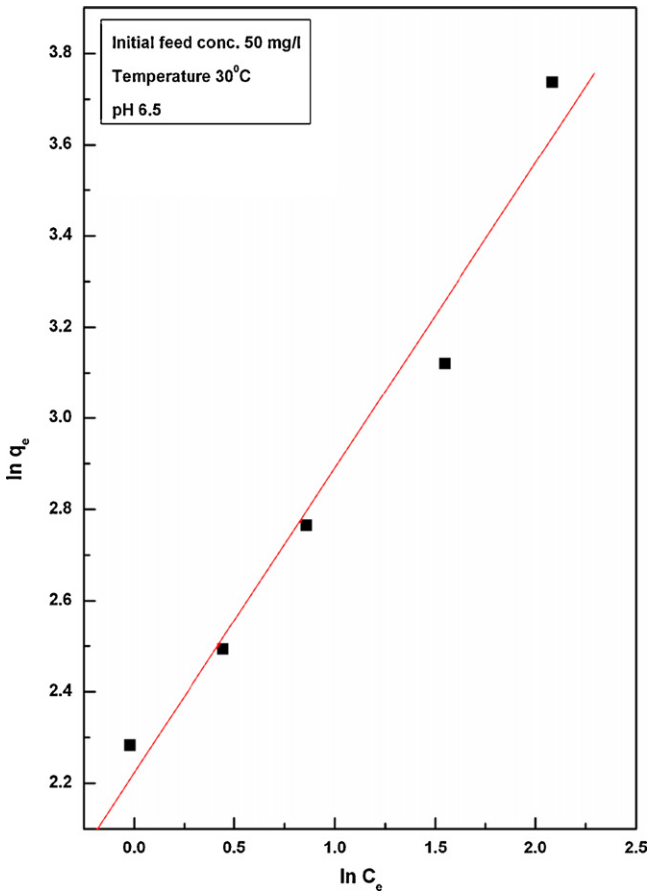

Fig. 16. Freundlich adsorption isotherm.

show that the rate of transfer of mass from bulk solution to the adsorbent surface was rapid enough so it cannot be rate controlling step [29]. It can also be mentioned that the deviation of some of the points from the linearity of the plots indicated the varying extent of mass transfer at the initial and final stages of the sorption.

3.5. Adsorption isotherms

Several models have been used in the literature to describe the experimental data of adsorption isotherms. The Freundlich and Langmuir models are the most frequently employed models. In the present work both models were used.

The lead(II) sorption isotherm followed the linearized Freundlich model as shown in Fig. 16. The relation between the metal uptake capacity 'q_e' (mg/g) of adsorbent and the residual metal ion concentration 'C_e' (mg/l) at equilibrium is given by

$$\ln\ q_e = \ln k + \frac{1}{n}\ln C_e \tag{12}$$

where the intercept $\ln k$ is a measure of adsorbent capacity, and the slope $1/n$ is the sorption intensity. The isotherm data fit the Freundlich model well ($R^2 = 0.984$). The values of the constants k and $1/n$ were calculated to be 9.231 and 0.668, respectively. Since the value of $1/n$ is less than 1, it indicates a favorable adsorption.

The Langmuir equation relates solid phase adsorbate concentration (q_e), the uptake, to the equilibrium liquid concentration (C_e) as follows:

$$q_e = \left(\frac{K_L b C_e}{1 + bC_e}\right). \tag{13}$$

where K_L and b are the Langmuir constants, representing the maximum adsorption capacity for the solid phase loading and the energy constant related to the heat of adsorption respectively. It can be seen from Fig. 17 that the isotherm data fits the Langmuir equation well ($R^2 = 0.973$). The values of K_L and b were determined from the figure and were found to be 43.859 mg/g and 0.274 l/mg, respectively. The outcome values of parameters k, n, K_L, b, R^2 for all the experiments with pH of solution equal to 6.5 for maximum removal of Pb(II) are presented in Table 2.

3.6. Effect of temperature on lead adsorption

Experiments were performed at different temperatures 10, 20, 30, 40 and 50 °C for different initial feed concentration and at constant adsorbent dose 2 g/l and pH of 6.5. The adsorption increased from 78.3 to 99.15, 73.8 to 96.4, 67.8 to 94.7 and 59.5 to 93.3% for different initial feed concentration 10, 20, 30 and 50 respectively with the rise in temperature from 10 to 50 °C (Fig. 18). It can be seen

Table 2
Adsorption isotherms parameter at pH 6.5 and temperature = 30 °C for Pb(II) removal.

Parameters	Values
K_L (mg/g)	43.859
b (l/g)	0.274
R^2	0.973 Langmuir, 0.984 Freundlich
K (1/g)	9.231
$1/n$	0.668

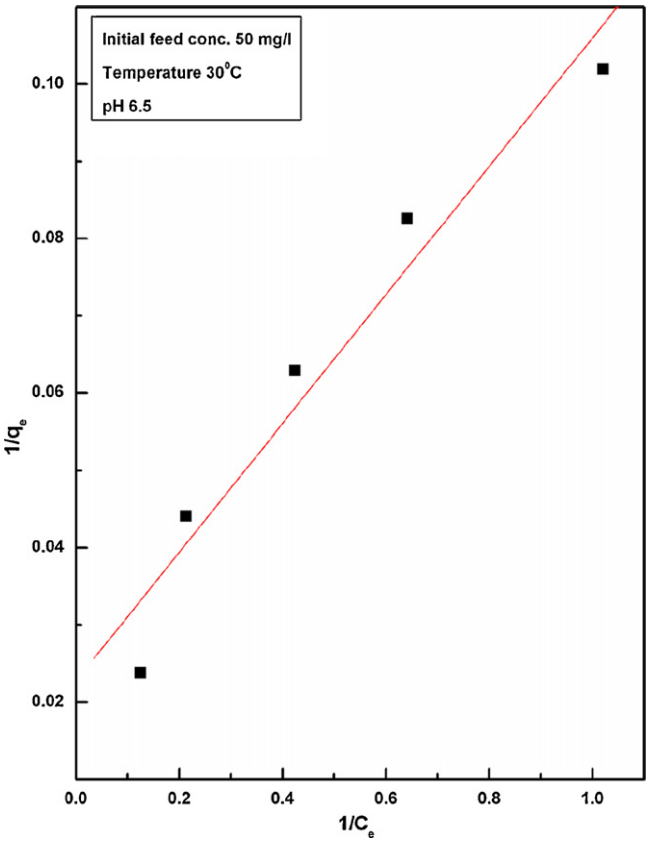

Fig. 17. Langmuir adsorption isotherm.

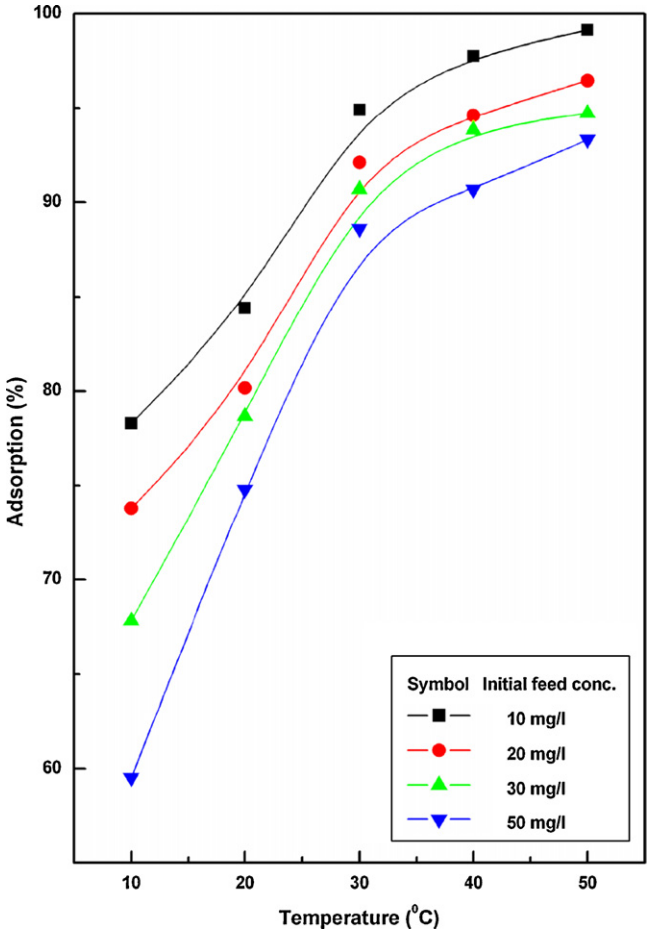

Fig. 18. Effect of temperature for different initial feed concentration at constant adsorbent dose 2 g/l and pH 6.5.

from the figure that initially the percentage removal increases very sharply with the increase in temperature but beyond a certain value 30–40 °C, the percentage removal reaches almost a constant value. The above results also showed that, the sorption was endothermic in nature. Since sorbent is porous in nature and possibilities of diffusion of sorbate cannot be ruled out therefore, increase in the sorption with the rise of temperature may be diffusion controlled which is endothermic process, i.e. the rise of temperatures favors the sorbate transport with in the pores of sorbent The increased sorption with the rise of temperature is also due to the increase in the number of the sorption sites generated because of breaking of some internal bonds near the edge of active surface sites of sorbent.

3.6.1. Thermodynamic parameters

Thermodynamic parameters such as free energy (ΔG°), enthalpy (ΔH°) and entropy (ΔS° change of adsorption can be evaluated from the following equations [14,15]:

$$K_c = \frac{C_{Ae}}{C_e} \tag{14}$$

$$\Delta G_0 = -RT \ln K_c \tag{15}$$

where K_c is the equilibrium constant and C_{Ae} and C_e (both in mg/l) are the equilibrium concentrations for solute on the sorbent and in the solution, respectively. The K_c values are used in Eqs. (14) and (15) to determine the ΔG°, ΔH° and ΔS° The K_c may be expressed in terms of the ΔH° (kJ mol^{-1}) and ΔS° (cal mol^{-1} K^{-1}) as a function of temperature:

$$\ln K_c = -\frac{\Delta H^\circ}{RT} + \frac{\Delta S^\circ}{R} \tag{16}$$

Thermodynamic parameters such as free energy of sorption (ΔG°), the heat of sorption (ΔH°) and standard entropy (ΔS°) changes during the sorption process were calculated using Eqs. (14)–(16) on a temperature range of 10–50 °C at different initial feed concentration of Pb(II), (ΔH°) and (ΔS°) and were obtained from the slope and intercept of a plot of $\ln K_c$ against $1/T$ (Fig. 19). The values of these parameters are recorded in Table 3. The negative values of ΔG° indicate the spontaneous nature of the process and more neg-

Table 3
Thermodynamic parameters for the adsorption of Pb(II).

C_0 (mg/l)	ΔH° (kJ mol^{-1})	ΔS° (kJ mol^{-1} K^{-1})	ΔG° (kJ mol^{-1})				
			10 °C	20 °C	30 °C	40 °C	50 °C
10	68.438	0.2503	−139.29	−141.79	−144.29	−146.80	−149.30
20	45.701	0.1812	−93.68	−95.37	−97.07	−98.76	−100.46
30	43.632	0.1465	−89.15	−90.76	−92.37	−93.98	−95.58
50	43.546	0.1580	−88.27	−89.85	−91.43	−93.01	−94.59

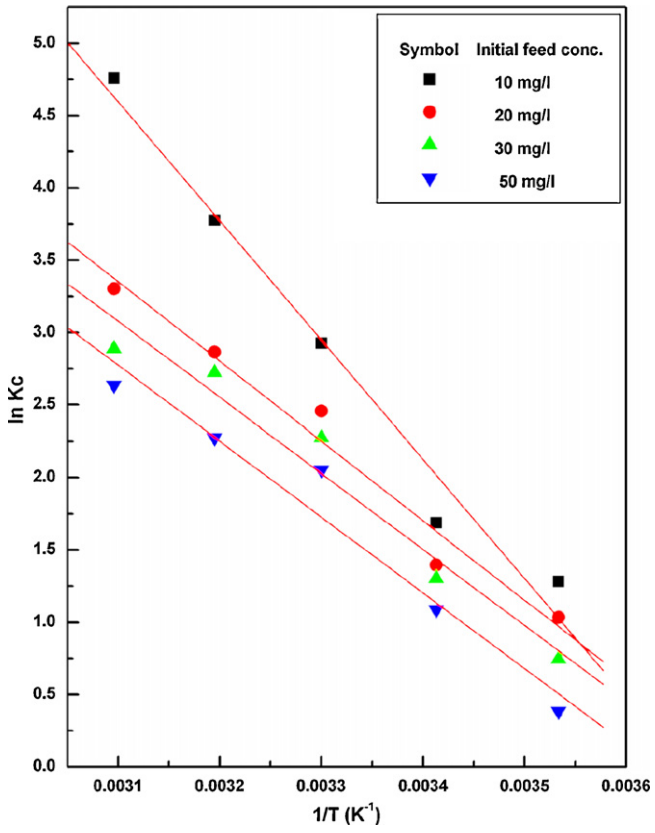

Fig. 19. A plot of $\ln K_c$ against $1/T$ for Pb(II) adsorption for different initial feed concentration at constant adsorbent dose 2 g/l and pH 6.5.

ative value with increase of temperature shows that an increase in temperature favors the sorption process. The positive values of ΔH° indicate that the sorption process was endothermic in nature and the negative values of ΔS° suggest the probability of a favorable sorption.

4. Conclusions

Removal of lead(II) from aqueous solutions is possible using several abundantly available low-cost adsorbents. The present investigation shows that *Tamarind wood* activated carbon is an effective adsorbent for the removal of lead(II) from aqueous solutions. Characterization has shown a clear demarcation in the physico-chemical properties of the adsorbent. From the kinetics studies it is observed that adsorption of lead(II) is very rapid in the initial stage and decreases while approaching equilibrium. The equilibrium time increases with initial lead(II) concentration. The percentage removal of lead(II) increases with the increase in adsorbent dosage and decrease with increase in initial lead(II) concentration. Experimental results are in good agreement with Langmuir adsorption isotherm model, and have shown a better fitting to the experimental data. Adsorption of lead(II) obeys pseudo-second-order equation with good correlation. The overall rate of lead(II) uptake was found to be controlled by pore diffusion, film diffusion and particle diffusion, throughout the entire adsorption period. Boyd plot confirmed that external mass transfer was the rate-limiting step in the sorption process. Different thermodynamic parameters, viz., ΔH°, ΔS° and ΔG° have also been evaluated and it has been found that the sorption was feasible, spontaneous and endothermic in nature. The positive value of the entropy change suggests the increased randomness. Under the prevailing conditions, the maximum Pb(II) removal efficiency was found to be 99%. As the adsorbent is derived from an agricultural waste, activated carbon may be useful for the economic treatment of wastewater containing lead(II). However, more investigations are needed on different types of industrial wastewaters and different operating conditions before such conclusions can be generalized.

References

[1] R. Jalali, H. Ghafourian, Y. Asef, S.J. Davarpanah, S. Sepehr, Removal and recovery of lead using nonliving biomass of marine algae, J. Hazard. Mater. B92 (2002) 253–262.
[2] V.K. Gupta, M. Gupta, S. Sharma, Process development for the removal of lead and lead from aqueous solutions using red mud-an aluminium industry waste, Water Res. 35 (5) (2001) 1125–1134.
[3] K. Conrad, H.C.B. Hansen, Sorption of zinc and lead on coir, Bioresour. Technol. 98 (1) (2007) 89–97.
[4] A. Groffman, S. Peterson, D. Brookins, Removing lead from wastewater using zeolites, Water Environ. Technol. 5 (1992) 54–59.
[5] I.S.I., Tolerance limits for industrial effluents prescribed by Indian Standards Institution, IS: 2490 (Part II), New Delhi, India, 1982.
[6] I.S.I., Drinking water specification prescribed by Indian Standards Institution, IS: 10500, New Delhi, India, 1991.
[7] M.M. Husein, J.H. Vera, M.E. Weber, Removal of lead from aqueous solutions with sodium caprate, Sep. Sci. Technol. 33 (12) (1998) 1889–1904.
[8] S.W. Lin, R.M.F. Navarro, An innovative method for removing Hg^{2+} and Pb^{2+} in ppm concentrations from aqueous media, Chemosphere 39 (11) (1999) 1809–1817.
[9] D. Petruzzelli, M. Pagano, G. Tiravanti, R. Passino, Lead removal and recovery from battery wastewaters by natural zeolite clinoptilolite, Solvent Extract. Ion Exch. 17 (3) (1999) 677–694.
[10] A. Saeed, M. Iqbal, M.W. Akhtar, Removal and recovery of lead(II) from single and multimetal (Cd, Cu, Ni, Zn) solutions by crop milling waste (black gram husk), J. Hazard. Mater. 117 (1) (2005) 65–73.
[11] S. Doyurum, A. Celik, Pb(II) and Cd(II) removal from aqueous solutions by olive cake, J. Hazard. Mater. 138 (1) (2006) 22–28.
[12] C.P. Dwivedi, J.N. Sahu, C.R. Mohanty, B. Raj Mohan, B.C. Meikap, Column performance of granular activated carbon packed bed for Pb(II) removal, J. Hazard. Mater. 156 (1–3) (2008) 596–603.
[13] C.K. Singh, J.N. Sahu, K.K. Mahalik, C.R. Mohanty, B. Raj Mohan, B.C. Meikap, Studies on the removal of Pb(II) from wastewater by activated carbon developed from Tamarind wood activated with sulphuric acid, J. Hazard. Mater. 153 (2008) 221–228.
[14] J.N. Sahu, S. Agarwal, B.C. Meikap, M.N. Biswas, Performance of a modified multi-stage bubble column reactor for lead(II) and biological oxygen demand removal from wastewater using activated rice husk, J. Hazard. Mater. 161 (1) (2009) 317–324.
[15] J. Goel, K. Kadirvelu, C. Rajagopal, V.K. Garg, Removal of lead(II) by adsorption using treated granular activated carbon: batch and column studies, J. Hazard. Mater. 125 (2005) 211–220.
[16] G. Issabayeva, K.M. Aroua, N.M.N. Sulaiman, Removal of lead from aqueous solutions on palm shell activated carbon, Bioresour. Technol. 97 (18) (2006) 2350–2355.
[17] N. Kannan, J. Balamurugan, Removal of lead ions by adsorption onto coconut shell and dates nut carbons—a comparative study, Indian J. Environ. Prot. 25 (9) (2005) 816–823.
[18] N. Kannan, M.S. Devi, Studies on removal of copper (II) and lead (II) ions by adsorption on commercial activated carbon, Indian J. Environ. Prot. 25 (1) (2005) 28–37.
[19] A. Garcia-Garcia, A. Gregoria, C. Francio, F. Pinto, D. Boavida, I. Gulyurtlu, Unconverted chars obtained during biomass gasification on a pilot-scale gasifier as a source of activated carbon production, Bioresour. Technol. 88 (2003) 27–32.
[20] A.C. Lua, J. Guo, Chars pyrolyzed from oil palm waste for activated carbon preparation, J. Environ. Eng. (1999) 72–76.
[21] M.G. Lussier, J.C. Shull, D.J. Miller, Activated carbons from cherry stones, Carbon 32 (8) (1994) 1493–1498.
[22] W. Su, L. Zhou, Y. Zhou, Preparation of microporous activated carbon from coconut shells without activating agents, Letters to the Editor, Carbon 41 (4) (2003) 861–863.
[23] C.J. Kirubakaran, K. Krishnaiah, S.K. Seshadri, Experimental study of the production of activated carbon from coconut shells in a fluidized bed reactor, Ind. Eng. Chem. Res. 30 (11) (1991) 2411–2416.
[24] D. Mohan, K.P. Singh, Single- and multi-component adsorption of cadmium and zinc using activated carbon derived from bagasse—an agricultural waste, Water Res. 36 (9) (2002) 2304–2318.
[25] K.A. Krishnan, T.S. Anirudhan, A preliminary examination of the adsorption characteristics of Pb(II) ions using sulfurized activated carbon prepared from bagasse pitch, Indian J. Chem. Technol. 9 (1) (2002) 32–40.
[26] J.-W. Kim, M.-H. Sohn, D.-S. Kim, S.-M. Sohn, Y.-S. Kwon, Production of granular activated carbon from waste walnut shell and its adsorption characteristics for CU^{+2} ion, J. Hazard. Mater. 85 (2001) 301–315.

[27] S. Ricordel, S. Taha, I. Cisse, G. Dorange, Heavy metals removal by adsorption onto peanut husks carbon: characterization, kinetic study and modeling, Sep. Purif. Technol. 24 (3) (2001) 389–401.
[28] C. Namasivayam, D. Sangeetha, Equilibrium and kinetic studies of adsorption of phosphate onto $ZnCl_2$ activated coir pith carbon, J. Colloid Interface Sci. 280 (2004) 359–365.
[29] K. Kadrivelu, K. Thamaraiselvi, C. Namasivayam, Adsorption of nickel(II) from aqueous solution onto activated carbon prepared from coirpith, Sep. Purif. Technol. 24 (3) (2001) 497–505.
[30] K. Srinivasan, N. Balasubramaniam, T.V. Ramakrishnan, Studies on lead removal by rice husk carbon, Indian J. Environ. Health 30 (4) (1988) 376–387.
[31] K. Mohanty, M. Jha, B.C. Meikap, M.N. Biswas, Removal of chromium (VI) from dilute aqueous solutions by activated carbon developed from *Terminalia arjuna* nuts activated with zinc chloride, Chem. Eng. Sci. 60 (2005) 3049–3059.
[32] A. Ahmadpour, D.D. Do, The preparation of activated carbon from Macademia Nutshell by chemical activation, Carbon 35 (12) (1997) 1723–1732.
[33] M. Al-Ghouti, M.A.M. Khraisheh, S. Allen, M.N.M. Ahmad, The removal of dyes from textile wastewater: a study of the physical characteristics and adsorption mechanisms of diatomaceous earth, J. Environ. Manage. 69 (2003) 229–238.